

# DEVELOPMENT OF FORGING PROCESS FOR SYNCHRONIZED RING THROUGH NUMERICAL SIMULATION

Papineni Satheesh<sup>1</sup>, \*N. S. Mahesh<sup>1</sup>, Bikas Musib<sup>2</sup>

<sup>1</sup> Department of Mechanical and Manufacturing Engineering, M. S. Ramaiah School of Advanced Studies, Bangalore,

<sup>2</sup> Manager, Advanced Forming Technology Centre (AFTC), Bangalore

\*Contact Author e-mail: nsm@msrsas.org

---

## Abstract

*Synchronized ring gear is the transmission mechanism in gearbox helping in shifting gears up from the second gear to the third gear. The transmission shift feeling is one of the important elements influencing the evaluation of vehicle controllability and operational comfort. During gear shifting maximum load will be on gear teeth. There is a chance of breakage if the gear teeth design and its microstructure is not good. Hence, manufacturing of these components will play a major role in maintaining the dimension and structural integrity of the component. It has been found from literature that many of automotive synchronized ring gear components are produced from forging process for specific advantages. In the present paper, an attempt has been made to develop hot forging process for synchronized ring through numerical simulation. Process modelling and simulation based on numerical method was used to iterate and to arrive at billet size, die design and process parameter selection.*

*3D model of forged component was developed using CATIA-V5 and gear teeth feature in the component was generated using Autodesk Inventor. Punch and die geometry was developed based on generated 3D model. Finite element based process modelling tool DEFORM was adopted for carrying out process simulation. FE model was generated using this tool. Forging force calculation was done from first principles and forging design guideline. This was done in order to arrive at press capacity required to form the part. Forging press capacity was finalized based on the force calculation and available press in the industry. The press selected for present study was 5 tonnes. Simulation was carried for 1/3<sup>rd</sup> of the component and finally achieved force was multiplied by 3. Effective stress and strain plots were obtained and ensured that the values are not crossing the fracture limits. Forging simulation was carried out at various temperatures within the range of hot working and appropriate working temperature was suggested. Microstructure evolution was also modelled to quantify the grain refinement, grain orientation*

**Keywords:** Numerical simulation, Process modeling, Finite Element Model, Microstructure evaluation

---

## Nomenclature

A	Projected area of forging (including the flash)
F	Forging load, mm <sup>2</sup>
Kp	Pressure multiplying factor
Tf	Flash thickness
$\sigma_f$	Flow stress of the material
V	Part Volume

## Abbreviations

FEM	Finite Element Method
SRX	Static Recrystallization
SD	Standard Deviation

## 1. INTRODUCTION

Metal forming is a process that has been constantly revolutionizing and evolving along with man since the conception of fire [1]. Throughout its history, metal forming has been an inadvertent sign of wealth, technology and power. Finally, today's outputs of automotive, aerospace and industrial products are controlled by the countries that are producing the majority of accurate metal parts using the most cost efficient process control.

Even though forging is not a new science, it has been forever evolving with the help of supercomputers and finite element modeling. Recently, it has become a more popular and inexpensive way of crafting net shaped and near net shaped metal products with less

design time and cost. With advances in technology, the spectrum of physical size products being generated is becoming larger with smaller design tolerances [2].

Forging is preferred in the industry because of some basic advantages as reduced machining operations, ability of producing complex parts, refined grain structure and optimum grain flow leading to desirable directional properties. In forging, there are no voids and porosity, have relatively uniform mechanical properties and also the response to heat treatment is predictable [1].

## 2. METHODOLOGY

Literature review on synchronized ring forging processes and process parameters and forging design guidelines was carried out extensively. The forging drawings and tooling drawings were developed based on design guidelines and industrial practices using CATIA-V5. Later, the production capacity, production requirements and quality of the product were analyzed for forging equipment selection. The required process flow for forging was developed based on the available press capacity and literature.

The process parameters were selected through iterative approach using process simulation tool, DEFORM and the validation was carried out with numerical trials.

### 3. MODEL CONSTRUCTION AND SOLUTION

#### 3.1 Development of forging drawings

2-D drawings of forged component were obtained and part features are shown in Table 1. 3-D models were developed using CATIA-V5 and Auto Desk Inventor. Developed models are shown in the Figure 1.

**Table 1. Forged Component Features**

Feature	Dimension in 'mm'
Number of Teeth	51
Pitch circle Diameter	153
Pressure angle	20°
Base circle Diameter	143.77
Internal Diameter	114.28
Outer Diameter	148.81
Thickness	16.1
Maximum wall thickness	6.6
Minimum wall thickness	1.5

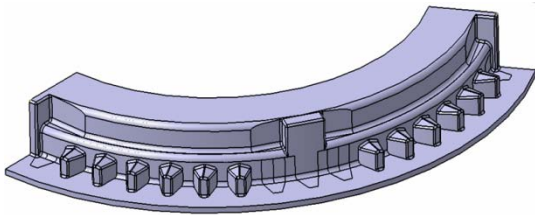


**Fig. 1 MIC 1066 Plastic Diesel Filter**

#### 3.2 Development of Tooling Drawings

3-D modelling software CATIA-V5 was used to model the dies. Volume of the drawn part was found and Boolean operation was performed by which specific shape can be subtracted or added to the other shape. For the component under study, Boolean operation was performed and die geometry was obtained through subtracting the forging component shape from a block. Top and bottom dies are shown in Figure 2a, 2b and 2c respectively. The largest diameter of the component was considered for extracting the die dimensions and smaller diameter was considered for extracting the punch dimensions in CATIA.

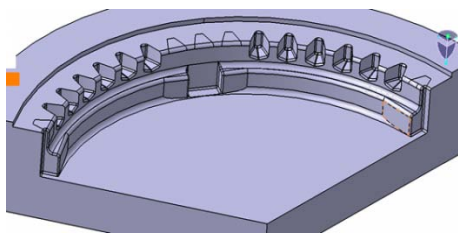


**Fig. 2a Developed tooling models - die (cavity) portion**

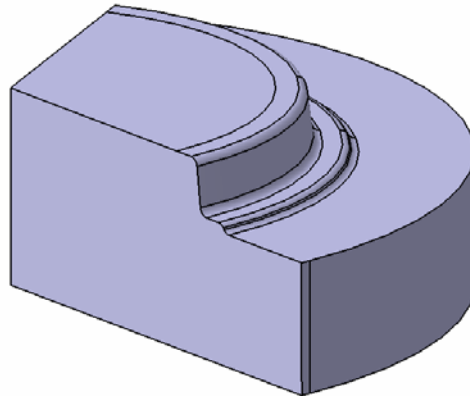


**Fig. 2b Developed tooling models - punch portion**

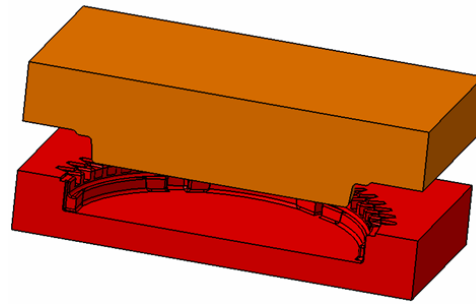


**Fig. 2c Assembly drawing of punch and the die**

#### 3.3 Forging Force Calculation

One of the considerations in bulk deformation problem is the size of the press needed for deformation. This requires the determination of the amount of force needed to cause the required deformation, which in turn requires the flow stresses and pressure to form the product. Accurate calculation of forces in impression-die forging is difficult. To simplify force calculation pressure, multiplying factor  $K_p$  is recommended [2].

$$F = K_p \sigma_f A$$

Where  $F$  is the forging load,  $A$  is the projected area of the forging (including the flash), and  $\sigma_f$  is the flow stress of the material. Typical  $K_p$  ranges are shown in Table 2.

**Table 2. Pressure multiplying factors [3]**

Pressure multiplying factors for closed die forging	
Forging Shape	$K_p$
Simple shapes, without flash	3-5
Simple shapes, with flash	5-8
Complex shapes, with flash	8-12

The forging material under study is 20MnCr5 and its flow stress ( $\sigma_f$ ) at 1320°C is  $52.05 \times 10^6$  N/m<sup>2</sup>. The flow stress value has been taken from DEFORM material property database exclusively available at various working temperatures. According to forging geometry, pressure-multiplying factor ( $K_p$ ) was selected as 8 and projected area ( $A$ ) of the forging including flash 0.013 m<sup>2</sup> (1/3<sup>rd</sup> of total projected area). The calculated forging force required to deform the material without considering any losses was found to be  $5.41 \times 10^6$  N.

### 3.4 Flash Thickness Calculation

The empirical formula for calculating the flash thickness ( $T_f$ ) is given by

$$T_f = 1.13 + 0.0789V^{0.5} - 0.000134V \dots\dots(1)$$

Where V is the part volume

Flash thickness was calculated to be 1.130 mm from equation 1. The flash thickness mentioned in the forging drawing given by the company was 1.5mm. Deviation in the flash thickness might be because of safety factors. Thus, the calculated flash thickness validates the die fill.

## 4. NUMERICAL SIMULATION

The process of synchronized ring hot forging involves complicated physical phenomenon in which the material plastic deformation is closely related to factors such as metal flow pattern, contact friction between blank and die, thermal conduction, microstructure and performance, etc. Therefore, it is very difficult to make predictions of material behaviour (deformation behaviour) during the forging process. Traditional ways of deciding preform shape and die design are dependent on either practical experience or trial-and-error method. The final design decision can only be made through multiple shop floor trials and modification, which often require prolonged lead-time.

### 4.1 Finite Element modelling of Synchronized Ring

DEFORM-3D is a FEM based deformation process modelling tool which can be helpful in validating the forging process design. This software has been used to analyse precision forging process of synchronized ring. With this package forging process can be simulated and various dies can be evaluated. Appropriate die set for which die cavity fills completely while maintaining a lower stress can be selected.

#### 4.1.1 Analysis in DEFORM-3D

Synchronized ring gear was formed using closed die forging. The factors considered in FE-process simulation are:

- Elastic deformation was assumed to be negligible and all the dies were regarded as the rigid bodies and the billet as the deformed body
- The friction at the billet-dies interfaces were assumed to be of shear type [4].
- The initial tetrahedral solid elements were around 100000 and automatic re-meshing technique was adopted during simulation and meshed dies. Initial billet models are shown in the Figure 3a meshed punch, 3b meshed die and 3c meshed initial billet.
- The billet material was given as 20MnCr5, and the die material was taken as AISI-H13

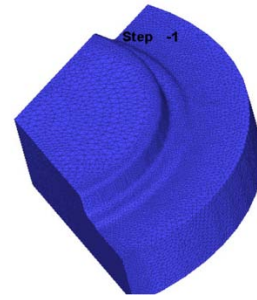


Fig. 3a Meshed punch portion



Fig. 3b Meshed die portion

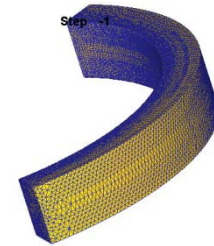
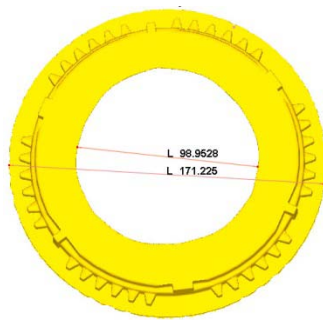


Fig. 3c Meshed billet portion

- Considering the practical conditions in the shop floor, the temperature of the dies and the environment was assumed as 150°C and 200°C, respectively
- The lead screw pitch of forging press - 330mm/rev and moment of inertia is  $5.7E10^6 \text{Nmm}^2$
- Heat transfer was allowed to cross the boundary between the billet and the dies and heat transfer coefficient was taken as 11
- Forging press capacity was fixed based on the available press in the industry that is  $4.8E10^8 \text{Nmm}$
- Initial trials were conducted with maximum available force and least available force to select the appropriate force.
- Initial billet temperatures were selected as 0.6% to 0.8% of melting temperatures of the material
- Simulation was carried for 1/3<sup>rd</sup> of the component and finally achieved force was multiplied by 3. Simulated model with an initial billet to the final deformed model are shown in Figure 3d and simulation trial report shown in Figure 3e.





**Fig. 5d Simulation trial-3: Exceeded internal diameter**

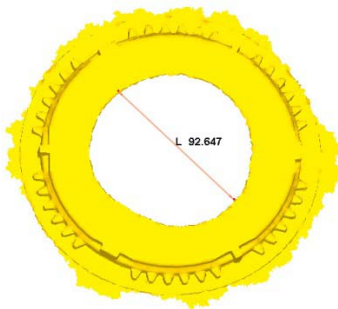


**Fig. 5e Simulation trial-4: Excess material flow**

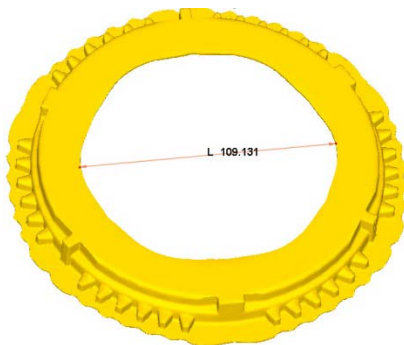


**Fig. 5f Simulation trial -5: Finalized billet size with less flash loss**

### 5.2 Influence of Forming Temperature

Selection of hot forging working temperatures was done based on material used and generic forging guidelines [6]. Working temperature was set as 0.6% to 0.8% of melting temperature of forged material.

Material 20MnCr5  
 Melting Point - 1400°C  
 Forging or  
 Preheating temp – 0.6 \* MP = 850°C  
 - 0.7 \* MP = 980°C  
 - 0.8 \* MP = 1120°C

Numerical trials were conducted with varying temperatures in above-mentioned ranges and trial report is shown in Figure 6.

Trial.no-	Forging Temperature- (°C)	Min, Max & Avg temperatures-(°C)	Billet size-(ID, OD, Thickness)	Standard deviation of Avg misorientation
1	850	762,1380,889	(128,148,16.5)	47.7
2	980	896,1270,1000	(128,148,16.5)	29.0
3	1120	1010,1340,1130	(128,148,16.5)	24.4

**Fig. 6 Temperature variations and their effect on process**

In the Figure 6, it can be observed that at 850°C standard deviation of temperature was 47.7°C and at 1120°C standard deviation was 24.4°C. While deforming, because of adiabatic heating at 850°C, maximum temperature variations are observed. If the cost of heating the dies can be observed, isothermal forging would be the best route for manufacturing. Since it helps to extend the die life. However, as an economical alternative, non-isothermal forging with die preheat of 150°C can be recommended.

### 5.3 Energy consumption according to temperatures

Energy consumed to deform the material will vary with initial billet temperature and the energy consumption trial report is shown in Figure 7a.

The inference from the energy consumption report was that when the temperature decreases, the energy consumption increases. Energy consumption plots according to temperatures shown in Figures 7b, 7c & 7d.

Trial. no-	Energy-consumption (N-mm)	Initial force-(N-mm)	Forging Temperature-(°C)	Billet size-(ID, OD, Thickness)	Remarks
1	7.3*10 <sup>6</sup>	4.5*10 <sup>8</sup>	850	(128,148,16.5)	Ok
2	5.64*10 <sup>6</sup>	4.8*10 <sup>8</sup>	980	(128,148,16.5)	Ok
3	4.31*10 <sup>6</sup>	2*10 <sup>8</sup>	1120	(128,148,16.5)	Ok
4	4.4*10 <sup>6</sup>	4.5*10 <sup>8</sup>	1120	(128,148,16.5)	Isothermal forging
5	15.9*10 <sup>6</sup>	4.8*10 <sup>8</sup>	20	(128,148,16.5)	Cold forging

**Fig. 7a Energy consumption report**

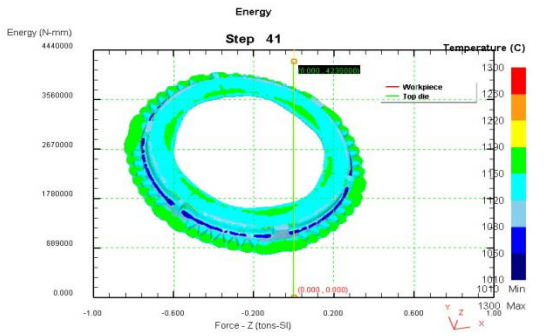


Fig. 7b Energy consumption at billet initial temperature - 1120°C

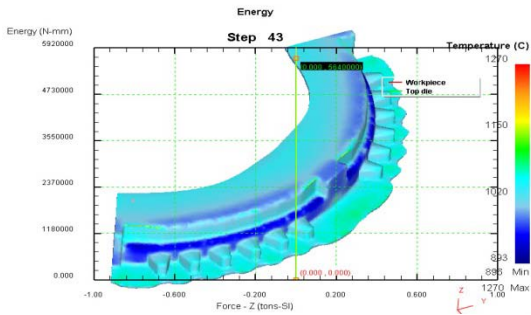


Fig. 7c Energy consumption at billet initial temperature - 980°C

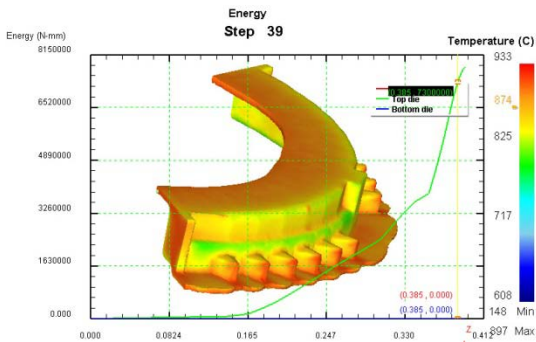


Fig. 7d Energy consumption at billet initial temperature 850°C

#### 5.4 Microstructure Evolution

During thermo-mechanical processing, significant changes in the microstructure are bound to happen. The changes can be recrystallization, grain refinement and change in phase [7]. In this paper, an attempt has been made to predict the resultant microstructure to understand its effect on mechanical properties.

Static recrystallization (SRX) grain growth model available in DEFORM has been used for carrying out trials because crystallization occurs after deformation in which the imposed strain is less than the critical strain. Recrystallization begins in a nucleus-free environment. Microstructure indicating grain size (min, max, avg. and SD), grain orientation at a given point in the geometry has been plotted. At selected points before deformation and after deformation microstructure variations were plotted. Figure 8a & 8b shows the

variation in grain size and 8c & 8d shows variation in grain orientation.

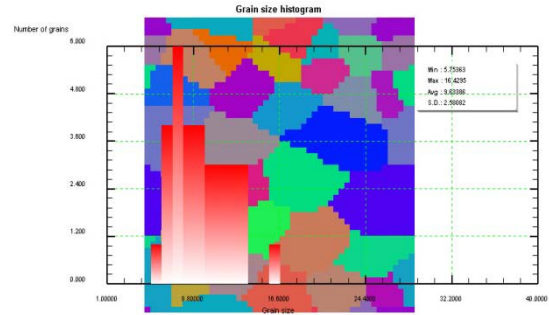


Fig. 8a Grain size before deformation at a selected point

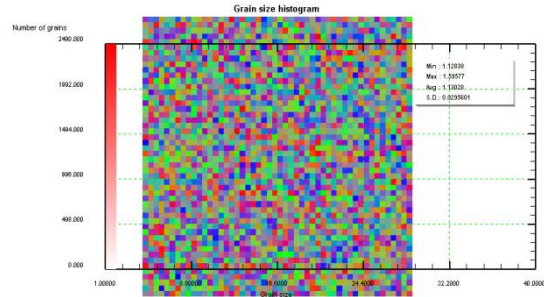


Fig. 8b Grain size after deformation at a selected point

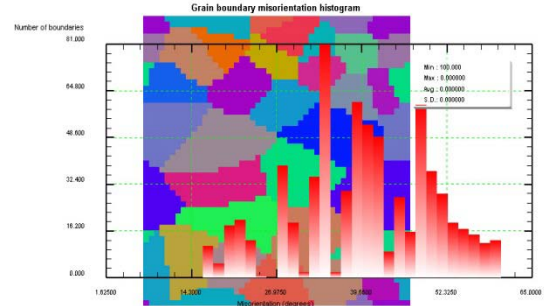


Fig. 8c Grain misorientation before deformation at selected point

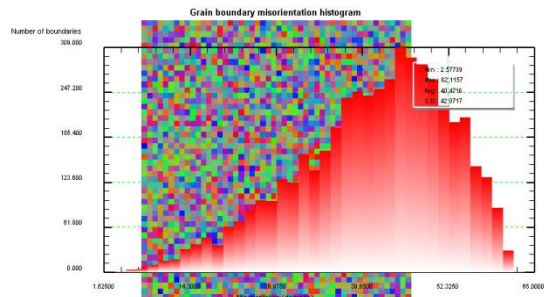


Fig. 8d Grain disorientation after deformation at selected point

Impacts of microstructure variation in forging for the selected points are shown in Figure 8e and 8f.

	Number of Grains						Average Grain Size (µm)							
	P1	P2	P3	P4	P5	P6	Range	P1	P2	P3	P4	P5	P6	S.D
Initial	6	5	7	6	6	7	5-7	9.63	9.70	9.64	9.74	9.69	9.74	2.13-3.08
Final	24	25	24	24	24	24	2490-2500	1.13	1.12	1.12	1.12	1.12	1.12	0-0.002

Fig. 8e Number of grains and grain size variation

	Number of Grains Boundaries						Average Misorientation (Deg)							
	P1	P2	P3	P4	P5	P6	Range	P1	P2	P3	P4	P5	P6	Range
Initial	81	65	76	70	72	82	65-82	0	0	0	0	0	0	Nil
Final	309	310	310	329	309	304	304-329	40.47	40.46	40.38	40.35	40.37	40.30	40.30-40.47

Fig. 8f Number of grain boundaries and disorientation

From Figure 8e, it can be observed before deformation the number of grains in the body ranges from 5-7 and after deformation the number of grains in the body ranges from 2490-2500. Standard deviation of the grain size before deformation was found to be  $2.13\mu\text{m}$  to  $3.08\mu\text{m}$  and after deformation 0 to  $0.002\mu\text{m}$ . The interference from the observed results indicates that homogeneity was improved after forging.

In Figure 8f it can be observed that the number of grain boundaries before deformation ranges from 65 to 82 and after deformation ranges from 304 to 329. Grain disorientation after deformation was observed to be 40.30 to 40.47. The interference from the observed results after forging dislocation in grain orientation were decreased and strength was increased.

### 5.5 Energy consumption according to billet size

According to billet size, the energy consumed to deform the material will vary [8] and by analysis of simulation results, it was observed that the increase in billet size would increase the energy consumption to deform the material.

### 5.6 Comparison of energy consumption according to temperatures

The energy consumed to deform the material was increasing with decrease in temperature. Results are shown in Figure 9.

T.no	Energy-consumption (N-mm)	Initial force- (N-mm)	Forging Temperature (°C)	Billet size- in mm (ID,OD,Thickness)	Remarks
1	$7.3 \times 10^6$	$4.5 \times 10^8$	850	(128,148,16.5)	Ok
2	$5.64 \times 10^6$	$4.8 \times 10^8$	980	(128,148,16.5)	Ok
3	$4.31 \times 10^6$	$2 \times 10^8$	1120	(128,148,16.5)	Ok
4	$4.4 \times 10^6$	$4.5 \times 10^8$	1120	(128,148,16.5)	Isothermal forging
5	$15.9 \times 10^6$	$4.8 \times 10^8$	20	(128,148,16.5)	Cold forging

Fig. 9 Energy consumption according to temperature

### 5.7 Microstructure variation according to temperatures

Microstructure, namely grain size and number of grain boundaries at a selected point in the deformed body based on working temperature are tabulated in 10a and 10b respectively. Analysis of the results showed that at  $1120^\circ\text{C}$  homogeneity in the microstructure was comparatively good.

After Deformation	Number of Grains						Average Grain Size (µm)							
	P1	P2	P3	P4	P5	P6	Range	P1	P2	P3	P4	P5	P6	Range
At 1120°c	2490	2500	2496	2494	2495	2498	2490-2500	1.13	1.12	1.12	1.12	1.12	1.12	1.12-1.13
At 980°c	2486	2483	2490	2489	2490	2480	2480-2490	1.12	1.12	1.12	1.13	1.12	1.12	1.12-1.13
At 850°c	2491	2301	2165	2050	2145	2275	2050-2491	1.12	1.16	1.19	1.22	1.20	1.17	1.12-1.22

Fig. 10a Grain size variation according to the temperatures

After Deformation	Number of Grains Boundaries						Average Misorientation (Deg)							
	P1	P2	P3	P4	P5	P6	Range	P1	P2	P3	P4	P5	P6	Range
At 1120°c	309	310	310	329	309	304	304-329	40.47	40.46	40.38	40.35	40.37	40.30	40.30-40.47
At 980°c	312	327	298	323	320	325	298-327	40.48	40.54	40.46	40.32	40.27	39.97	40.54-39.97
At 850°c	327	300	300	290	303	306	290-327	40.24	40.27	40.91	40.50	40.43	40.33	40.24-40.91

Fig. 10b Number of grain boundary variation to temperature

## 6. CONCLUSION

The aim of work was to develop forging process for a given component namely synchronized ring. Process modelling and simulation based on numerical method was used to iterate and to arrive at billet size, die design and process parameter selection. The summary of findings during the course of present study is:

- 3D model of forged component was developed using CATIA-v5 and gear teeth feature in the component was generated using Autodesk Inventor.
- Punch and die geometry was developed based on 3D model generated.
- Finite Element based process modeling tool DEFORM was adopted for carrying out process simulation. FE model was generated using this tool.
- Forging force calculation was done from first principles and forging design guideline. This was done to arrive at press capacity required to form the part. Forging press capacity was finalized based on the force calculation and available press in the industry. The press selected for present study was 5 tonnes.
- Simulation was carried for  $1/3^{\text{rd}}$  of the component and finally achieved force was multiplied by 3
- Effective stress and strain plots were obtained and ensured that the values are not crossing the fracture limits
- Forging simulation was carried out at various temperature within the range of hot working and appropriate working temperature was suggested
- Microstructure evolution was also modeled to quantify the grain refinement, grain orientation
- Figure 11 consolidates recommended hot forging parameters determined based on the present study

T.no	Energy-consumption (N-mm)	Initial force- (N-mm)	Forging Temperature (°C)	Billet size- in mm (ID,OD,Thickness)	Remarks
1	$4.31 \times 10^6$	$1.94 \times 10^8$	1120	(128,148,16.5)	Ok

Fig. 11 Recommended forging parameters

## 7. REFERENCES

- [1] Kalpakjian, Schmid, *Manufacturing Engineering and Technology for Metal-Forging Processes and Equipment*, [http://www.engr.mun.ca/~adfisher/3941/Ch14\\_Metal-Forging-HO.pdf](http://www.engr.mun.ca/~adfisher/3941/Ch14_Metal-Forging-HO.pdf), Retrieved on 17<sup>th</sup> Nov 2012.
- [2] Helmi A. Youssef, Hassan A., El- Hofy, *Manufacturing technology of bulk forming of metallic materials*.
- [3] ASM Speciality Handbook, Tool Steel Materials, Materials for Metal Working Application- Page 220.
- [4] Altan T., Shirgaokar M., Process Design in Impression Die Forging, <http://nsmwww.eng.ohio-state.edu/467.pdf>, Retrieved on 19<sup>th</sup> Dec 2012.
- [5] Randhir Kumar, Niranjana Kumar Singh, Rajkumar Ohdar, *Optimization of the Process Parameters of Semisolid Forging of A356 Aluminum Alloy*, <http://www.ijest.info/docs/IJEST12-04-03-007.pdf>, Retrieved on 14<sup>th</sup> sep 2012.
- [6] YI Youping, CUI Jindong, LIN Yongcheng, *Numerical simulation of process and grain size for large-sized aluminum alloy 7050 forging*, <http://ieeexplore.ieee.org/stamp/stamp.jsp?tp=&arnumber=4752032>, Retrieved on 27<sup>th</sup> sep 2012.
- [7] ASM Handbook, Volume 14, 9<sup>th</sup> Edition, Metals Handbook, Forming and Forging, page- 46.
- [8] Geoffrey Boothroyd and Peter Dewhurst, *Product Design for Manufacture and Assembly*, 3<sup>rd</sup> Edition